ELSEVIER

Journal of Alloys and Compounds 293–295 (1999) 742–746

Journal of ALLOYS AND COMPOUNDS

Comparison of the electrochemical properties of cast and melt-spun $MLNi_{4.3-x}Co_xMn_{0.4}Al_{0.3}$ (ML: La-rich Mischmetal) hydrogen-storage alloys

Chuan-Jian Li*, Xin-Lin Wang, Chong-Yu Wang

Advanced Materials Institute, Central Iron and Steel Research Institute, Beijing 100081, People's Republic of China

Abstract

A series of hydrogen-storage alloys of composition $MLNi_{4.3-x}Co_xMn_{0.4}Al_{0.3}$ (ML denotes Lanthanum-rich Mischmetal and, $x=0.2$, 0.4, 0.5, 0.6, 0.7 and 0.9) were prepared with two methods, conventional casting and melt-spinning. The electrochemical properties of these alloys were measured and compared. It was found that rapid quenching by melt-spinning could very effectively improve the cycle stability of the AB_5-type alloy, especially the cycle stability of the alloy with a low content of cobalt. Melt-spinning had some disadvantages in that it slowed down the initial activation rate and narrowed the width of the discharge voltage plateau and therefore led to a decrease in capacity. The phase structure of the investigated alloys was also measured by X-ray diffraction technique showing that all alloys were the same AB_5 phase with $CaCu_5$ structure.

Keywords: Hydrogen storage alloy; Melt-spun; Cast; Electrochemical property

1. Introduction

With the increasing demands for portable electronic devices, electric vehicles and an improvement of our living environment, the development of 'green batteries' becomes more and more important in the world. The nickel/metal hydride (Ni/MH) battery is one of the 'green batteries' which gives high rate capability, large capacity, long cycle life, no memory effect and no pollution. Therefore, hydrogen storage alloys as a kind of energy conversion materials have attracted world-wide interest. Various metals and intermetallic compounds and their hydrogen absorption/desorption feature have been widely investigated. The present studies have indicated that hydrogen storage ability, kinetics of hydrogen absorption–desorption, catalytic property, electrochemically discharge capacity, high-rate discharge capability and cycle durability as a negative electrode of Ni/MH battery are significantly influenced by the phase structure, microstructure, alloy composition and surface characteristics [1–20]. The Ni/MH battery using rare-earth-based alloys can meet the demands of the battery for electric vehicles, e.g. high energy density, high power density, long cycle life and maintenance-free operation and low-cost per cycle. However, in this alloy series, cobalt is the most important alloy element generally at a content of 10 wt.% in alloys in order to obtain good cycle stability of alloys; it amounts to almost 50% of the total cost of the raw materials. Because the price of cobalt in the world market fluctuates largely and is relatively high, it must affect negatively the production of AB_5-type alloys, especially the alloy used for vehicle battery which usually needs a large quantity of the hydrogen storage alloy per battery. Furthermore, cobalt can also decrease the high-rate discharge capability of the AB_5-type alloy. So, a decrease or elimination of cobalt in this kind of alloy is needed to enlarge its application and increase its competitive capability.

In previous works [21–23], rapid solidification of the melted alloy using melt-spinning technique proved to be very effective for increasing the cycle stability of various AB_5-type alloys. In the present work, the electrochemical properties of melt-spun alloys of different contents of cobalt were measured and compared with those of the

*Corresponding author. The present address: Department of Environmental and Chemical Engineering, Kogakuin University, Tokyo 192-0015, Japan.

0925-8388/99/$ – see front matter
PII: S0925-8388(99)00349-7

corresponding alloys prepared by conventional methods, i.e., casting.

2. Experimental

2.1. Preparation of the alloys

Alloys of compositions of $MLNi_{4.3-x}Co_xMn_{0.4}Al_{0.3}$ (ML denotes Lanthanum-rich Mischmetal and $x=0.2$, 0.4, 0.5, 0.6, 0.7 and 0.9) were prepared by arc melting the constituent elements under an argon atmosphere on a water-cooled copper crucible. Part of the each cast alloy was re-melted and rapidly quenched to flakes by a melt-spinning method with single copper wheel under an argon atmosphere. The surface velocity of the copper wheel was set to 35 ms^{-1}.

2.2. Alloy powder preparation

All alloys were pulverized mechanically to particle size under 70 μm for electrochemical property and X-ray powder diffraction measurements.

2.3. Electrode preparation and electrochemical measurement

Electrode pellets of 11 mm in diameter were prepared by mixing 1 g alloy powder with fine nickel powder in a weight ratio of 1:1 together with a small amount of polyvinyl alcohol (PVA) solution as a binder, followed by compressing at a pressure of 3500 kg cm^{-2} after vacuum drying at 80 for about 45 min. Before the electrochemical measurements, the sample electrodes were immersed in the electrolyte for at least 1 day in order to fully wet the electrode. To prevent the electrode plate from breaking into pieces during the charge–discharge cycling it was clamped and pressed by porous nickel. As counter- and reference electrodes, a sintered nickel hydroxide ($Ni(OH)_2$/NiOOH) plate and a Hg/HgO 6 M KOH electrode were employed respectively. Multiple constant charge/discharge currents were adopted for the measurements of the discharge capacity and the cycle life together with the discharge potential, which was described in detail in a previous paper [24]. The discharge was cut off at −0.500 V vs. Hg/HgO 6 M KOH. Every cycle was carried out by charging fully and discharging to −0.500 V with respect to a Hg/HgO 6 M KOH reference electrode at the environmental temperature of 25.

2.4. Phase structure determination

The phase structure of the alloy powders before charge–discharge cycling was identified by X-ray diffraction experiments with Co $K_{\alpha 1}$ or Cu $K_{\alpha 1}$ radiation.

Table 1
Characterization of the initial activation rate of the investigated alloys

Alloy composition $MLNi_{4.5-x}Co_xMn_{0.4}Ai_{0.3}$	$N_{60m,max}$(cycle)	
	as-cast	melt-spun
$x=0.2$	2	9
$x=0.4$	3	10
$x=0.5$	2	10
$x=0.6$	2	11
$x=0.7$	3	12
$x=0.9$	2	15

3. Results and discussion

3.1. Electrochemical properties of the investigated alloys

3.1.1. Activation of the alloys

The initial activation rate of the alloy is characterized by the cycle number $N_{60,max}$, at which the discharge capacity at a discharge rate of 60 mAg^{-1} reaches its maximum value in the earlier stage of the charge/discharge cycling. Obviously a smaller $N_{60,max}$ implies that the corresponding alloy is easier to activate. Table 1 gives the $N_{60,max}$ values for the different alloys of different compositions or prepared with different methods. From Table 1, all as-cast alloys were generally easier to activate and the $N_{60,max}$ was no more than 3 cycles and the content of cobalt had almost no influence on the initial activation rate of the as-cast alloy. However, all alloys became very difficult to activate after being quenched by melt-spinning and the content of cobalt had slight influence on the initial activation rate of the quenched alloys. From Table 1, it can be found that the melt-spun alloy with a lower content of cobalt could be more easily activated.

3.1.2. Discharge voltage characterization

As shown in Fig. 1, the discharge voltage plateau of melt-spun alloys were generally flatter than those of as-cast alloys, which has been found in our previous work [21].

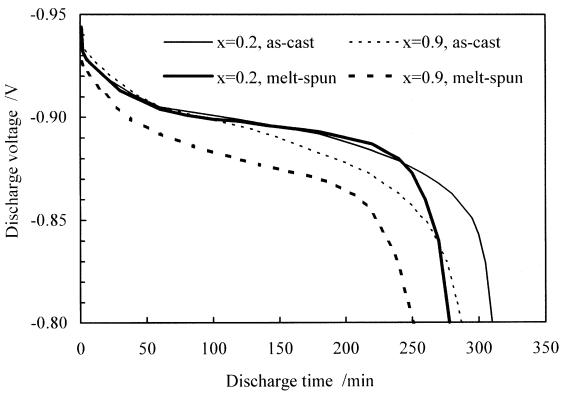

Fig. 1. Discharge voltage characteristics of electrodes made from the as-cast and melt-spun alloys at a constant discharge current of 60 mAg^{-1} at 25 (vs. Hg/HgO 6M KOH).

The flattened discharge voltage plateau came from the more homogeneous composition due to rapid quenching. It has been found that the rapid quenching process can flatten the plateau region of hydrogen absorption P-C isotherms at 313 K [31]. However, the width of the discharge plateau of melt-spun alloys were narrower than those of their corresponding as-cast alloys. The shortened discharge plateau led to a decrease in the discharge capacity, which would be discussed in detail later. It has been confirmed that the shortening of the plateau results from the existence of the amorphous phase introduced by rapid quenching [21]. A purely amorphous $LaNi_5$-type alloy has no discharge plateau [25–30]. The discharge plateau of the melt-spun alloy with a low content of cobalt, e.g. $x=0.2$, had nearly the same width as, but flatter than that of the cast alloy with a cobalt content $x=0.9$.

The discharge voltage characteristics of melt-spun alloys deteriorated with increasing cobalt content (Fig. 2). The melt-spun low-cobalt-content alloys (e.g. $x=0.2$ and 0.4) got very good discharge voltage performance curves even at a relatively high discharge rate of 300 mAg^{-1}.

3.1.3. Discharge capacity and high-rate discharge capability

Fig. 3 shows the discharge current dependence of the discharge capacity. The discharge capacity of all alloys decreased with increasing cobalt content, but this decrease was very limited. However, the capacity of alloys with different Co contents decreased to a much lower level after being quenched, especially for the capacity at the high discharge rate (e.g. 300 mAg^{-1}). The decrease in the capacity was consistent with the result mentioned above that the discharge voltage plateau was shortened after quenching. It is well known that the discharge capacity of the metal-hydride electrode decreased with increasing the discharge rate. The high-rate discharge capability of the alloy is better when the above reduction in capacity is less compared with that of other alloys. So, the high-rate discharge capability C_h can be defined as

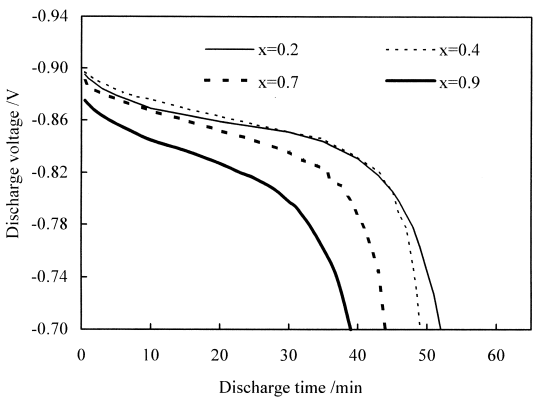

Fig. 2. Discharge voltage characteristics of electrodes made from melt-spun alloys with different Co contents at a constant discharge current of 300 mAg^{-1} at 25 (vs. Hg/HgO 6M KOH).

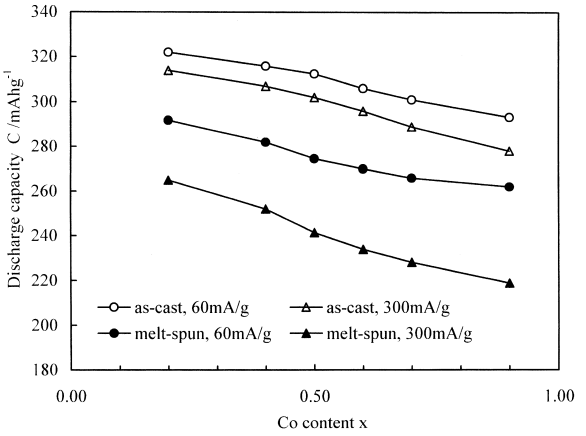

Fig. 3. Discharge capacity of alloy electrodes at different discharge currents.

$$C_h = \frac{C_{300}}{C_{60}} \times 100\%$$

where C_{300} and C_{60} are the maximum discharge capacities at discharge currents of 300 mAg^{-1} and 60 mAg^{-1}, respectively. The relations between the high-rate capability of alloys both in as-cast state and in as-quenched state and the cobalt content is illustrated in Fig. 4. From Fig. 4, it can be found that the high-rate capability varied with the cobalt content before and after quenching. The high-rate capability of melt-spun alloys decreased more rapidly with increasing cobalt content than that of as-cast alloys and, the former was generally lower than the latter which means that rapid quenching by melt-spinning led to a decrease in high-rate capability C_h.

3.1.4. Cycle stability

The capacity decay rate of the as-cast alloy decreased with increasing cobalt content (Fig. 5). From Fig. 5, cobalt played an important role in improving the cycle stability of the as-cast alloy. The cycle stability of the alloy with a low content of cobalt, $x=0.2$, was so poor that its capacity

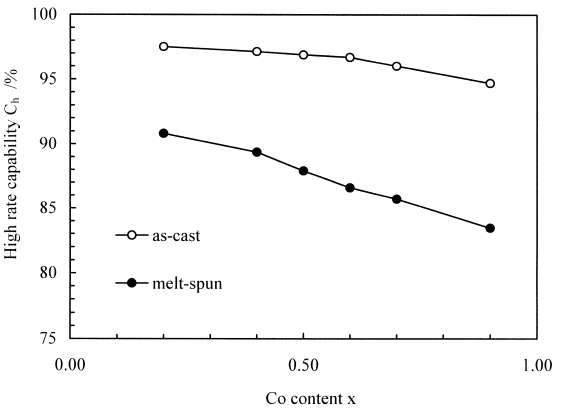

Fig. 4. The relations between the high-rate discharge capability and the Co content.

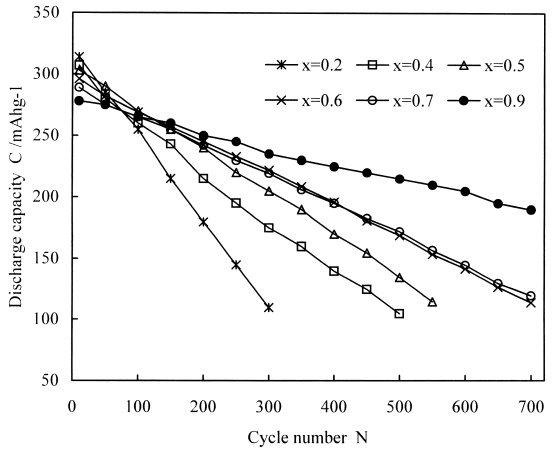

Fig. 5. Curves of the capacity at a discharge rate of 300 mAg^{-1} vs. cycle number for different as-cast alloy electrodes at 25.

decreased so rapidly that it was only about 110 $mAhg^{-1}$ after just 300 cycles. However, the cycle stability of all alloys was improved by a big margin after quenching treatment (Fig. 6). The capacity of the melt-spun alloy with a cobalt content $x=0.2$ still remained 190 $mAhg^{-1}$ though it had experienced 550 cycles.

Comparing Fig. 5 with Fig. 6, it is very clear that rapid quenching was more effective in improving the cycle stability of the low-cobalt alloy than the high-cobalt alloy. According to aforesaid experimental results, both the replacing of cobalt for nickel and rapid quenching led to a decrease in capacity and high-rate capability. However, it was reported that annealing at a proper temperature can compensate for the shortcomings of melt-spinning [24]. Annealing can increase the initial activation rate, the capacity, the high-rate capability, the height of the discharge voltage plateau and even further improving the cycle stability of the melt-spun alloy. So, melt-spinning

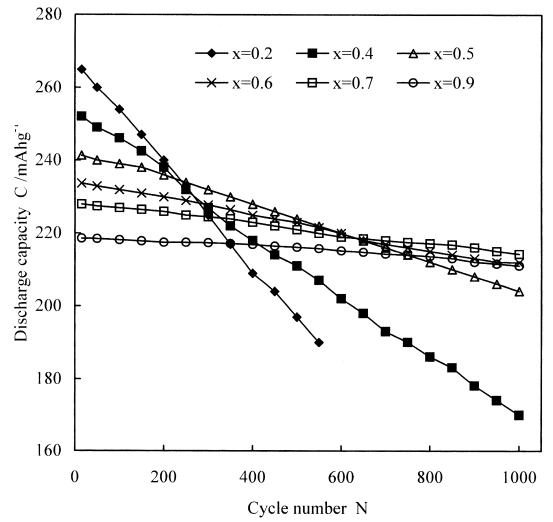

Fig. 6. Curves of the capacity at a discharge rate of 300 mAg^{-1} vs. cycle number for different melt-spun alloy electrodes at 25.

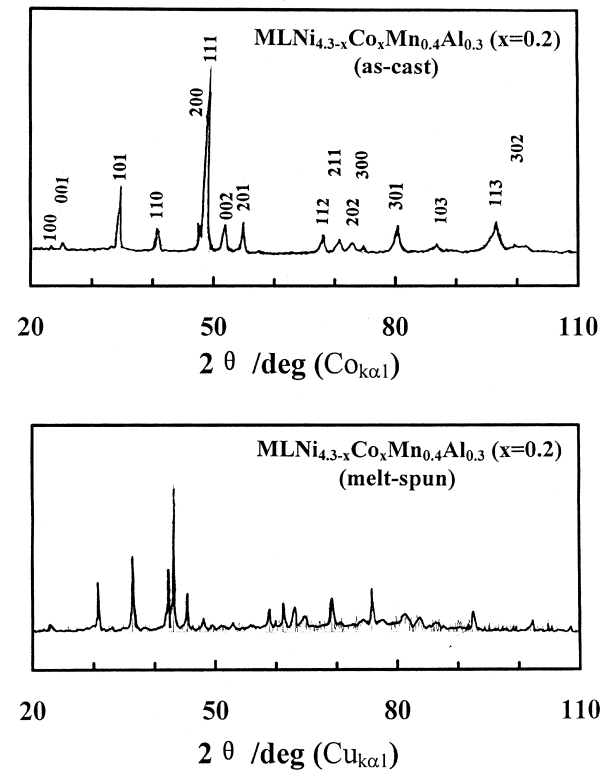

Fig. 7. XRD patterns for the alloy of composition $MLNi_{4.3-x}Co_xMn_{0.4}Al_{0.3}$ ($x=0.2$) before and after quenching.

can be used as a feasible method to produce low-cobalt-content or cobalt-free AB_5-type alloys with excellent cycle stability and synthetic electrochemical properties, which can reduce the cost of the raw materials by a big margin because the price of cobalt is very high compared with those of other alloy elements such as Mischmetal, Mn, Ni and Al, etc.

3.2. Phase structure

The phase structure of all the investigated alloys was determined using X-ray diffraction and all alloys can be indexed as AB_5-type phase with $CaCu_5$ structure. Different cobalt substitution for nickel and preparing method made no change to the phase structure. Two typical XRD patterns for the alloy of composition $MLNi_{4.3-x}Co_xMn_{0.4}Al_{0.3}$ ($x=0.2$) both in as-cast and as-quenched states were shown in Fig. 7. The structure of the investigated alloys will be further studied and the result reported in another paper [32].

4. Conclusion

A series of hydrogen-storage alloys of composition $MLNi_{4.3-x}Co_xMn_{0.4}Al_{0.3}$ (ML denotes Lanthanum-rich Mischmetal and, $x=0.2$, 0.4, 0.5, 0.6, 0.7 and 0.9) were prepared with two methods, conventional casting and melt-

spinning. The electrochemical properties and the phase structure of these alloys were measured and compared. The following conclusions were drawn:

1. Rapid quenching by melt-spinning could very effectively improve the cycle stability of the AB_5-type alloy, especially for the cycle stability of the alloy with a low content of cobalt.
2. Melt-spinning had some disadvantages in that it slowed down the initial activation rate and narrowed the width of the discharge voltage plateau and therefore led to a decrease in capacity.
3. The phase structure of the investigated alloys was also measured by X-ray diffraction technique showing that all alloys were the same AB_5 phase with $CaCu_5$ structure.
4. Melt-spinning can be used as a feasible method to produce low-cobalt or cobalt-free AB_5-type hydrogen storage alloys for electrode usage.

Acknowledgements

This work was supported by the National Advanced Materials Committee and the High Technology '863' Projects of the People's Republic of China under Contract No. 863-715-004-0230.

References

[1] J.J.G. Willems, Philips J. Res. 39 (suppl.1) (1984) 1.
[2] J.J.G. Willems, K.H.J. Buschow, J. Less-Common Met. 129 (1987) 13.
[3] H. Bjurström, S. Suda, J. Less-Common Met. 131 (1987) 61.
[4] S. Suda, Int. J. Hydrogen Energy 12 (1987) 323.
[5] Z.P. Li, S. Suda, J. Alloys Comp. 231 (1995) 751.
[6] F.-J. Liu, S. Suda, G. Sandrock, J. Alloys Comp. 232 (1996) 232.
[7] X.-L. Wang, K. Iwata, S. Suda, J. Alloys Comp. 231 (1995) 829.
[8] W.-K. Hu, Y.-S. Zhang, D.-Y. Song, P.-W. Shen, Int. J. Hydrogen Energy 21 (1996) 651.
[9] T. Sakai, K. Oguro, H. Miyamura, N. Kuriyama, A. Kato, H. Ishikawa, J. Less-Common Met. 161 (1990) 193.
[10] T. Sakai, H. Miyamura, N. Kuriyama, A. Kato, K. Oguro, H. Ishikawa, J. Less-Common Met. 159 (1990) 127.
[11] D. Chartouni, F. Meli, A. Züttel, K. Gross, L. Schlapbach, J. Alloys Comp. 241 (1996) 160.
[12] L. Jiang, F. Zhan, D. Bao, G. Qing, Y. Li, X. Wei, J. Alloys Comp. 231 (1995) 635.
[13] A. Züttel, D. Chartouni, K. Gross, P. Spatz, M. Bächler, F. Lichtenberg, A. Fölzer, N.J.E. Adrins, J. Alloys Comp. 253–254 (1997) 626.
[14] R.C. Bowman Jr., C. Witham, B. Fultz, B.V. Ratnakumar, T.W. Ellis, I.E. Anderson, J. Alloys Comp. 253–254 (1997) 613.
[15] Y.-M. Sun, K. Iwata, S. Chiba, Y. Matsuyama, S. Suda, J. Alloys Comp. 253–254 (1997) 520.
[16] K. Yasuda, J. Alloys Comp. 253–254 (1997) 621.
[17] T. Akiyama, T.A. Tazaki, R. Takahashi, J. Yaji, Intermetallics 4 (1996) 659.
[18] Y. Yang, J. Li, J.M. Nan, Z.G. Li, J. Power Sources 65 (1997) 15.
[19] F.-J. Liu, S. Suda, J. Alloys Comp. 232 (1996) 212.
[20] F.-J. Liu, S. Suda, J. Alloys Comp. 232 (1996) 204.
[21] C.-J. Li, X.-L. Wang, C.Y. Wang, J. Alloys Comp. 266 (1998) 300.
[22] C.-J. Li, X.-L. Wang, X.M. Li, C.Y. Wang, Electrochimica Acta 43 (1998) 1839.
[23] C.-J. Li, X.-L. Wang, C.Y. Wang, J. Power Sources 74 (1998) 62.
[24] C.-J. Li, X.-L. Wang, J.M. Wu, C.Y. Wang, J. Power Sources 70 (1998) 106.
[25] H. Sakaguchi, T. Suenobu, K. Moriuchi, M. Yamagami, T. Yamaguchi, G.-Y. Adachi, J. Alloys Comp. 221 (1995) 212.
[26] Y. Li, Y.-T. Cheng, J. Alloys Comp. 223 (1995) 6.
[27] G. Adachi, K.I. Niki, H. Nagai, J. Shimokawa, J. Less-Common Met. 88 (1988) 213.
[28] F.H.M. Spit, J.W. Drijver, W.C. Turkenurg, S. Radelaar, Scr. Metall. 14 (1980) 1071.
[29] R. Kirchheim, F. Sommer, G. Schluckebier, Acta Metall. 30 (1982) 1059.
[30] G.G. Libowitz, A.J. Mealand, J. Less-Common Met. 101 (1984) 131.
[31] N. Higashiyama, Y. Matsuura, H. Nakamura, M. Kimoto, M. Nogami, I. Yonezu, K. Nishio, J. Alloys Comp. 253–254 (1997) 648.
[32] C.-J. Li, X.-L. Wang, C.Y. Wang, J. Alloys Comp. (to be submitted).